

Zinc-Bound Thiolate–Disulfide Exchange: A Strategy for Inhibiting Metallo- β -lactamases

Heidi Boerzel, Margery Koeckert, Weiming Bu, Bernhard Spingler, and Stephen J. Lippard*

Department of Chemistry, Massachusetts Institute of Technology, Cambridge, Massachusetts 02139

Received March 31, 2002

The mononuclear zinc thiolate complexes [(Tp^{PhMe})Zn(S-R)], where Tp^{PhMe} is hydrotris((3-methyl-5-phenyl)pyrazolyl)borate and (S-R) is benzyl thiolate, 4-nitrophenylthiolate, 4-trifluoromethylphenylthiolate, 4-chlorophenylthiolate, phenylthiolate, 2-methylphenylthiolate, 4-methylphenylthiolate, 4-methoxyphenylthiolate, or 4-hydroxyphenylthiolate, were synthesized. Representative members of the class were also characterized structurally. The benzyl thiolate complex undergoes a thiolate–disulfide exchange reaction with a variety of diphenyl and dipyridyl disulfides. Kinetic studies revealed that the reaction shows saturation behavior in both complex and disulfide for most of the disulfides studied. Combined with studies of the lability of the coordinated thiolate, a mechanism is proposed where the reactive species is the zinc-coordinated thiolate. When the free benzyl thiol was allowed to react with the same disulfides, the reaction was slower by a factor of 20–200 than that for the zinc–thiolate complex, depending on the particular disulfide employed. Since most metallo- β -lactamases contain one or more cysteine residues, the one in the active site being coordinated to zinc, the present study was extended to examine whether disulfides can be used as inhibitors of these enzymes by selective oxidation of the metal-bound cysteine. Several disulfides allowed to react with metallo- β -lactamase CcrA from *Bacteroides fragilis* were moderate to potent irreversible inhibitors of the enzyme.

Introduction

Metallo- β -lactamases are currently emerging as major targets for overcoming bacterial drug resistance. In recent years, pathogens capable of producing metallo- β -lactamases have been isolated with increasing frequency.^{1,2} These enzymes contain mono- or dinuclear zinc centers that inactivate a wide range of β -lactam antibiotics by amide bond hydrolysis. Most of the current β -lactam antibiotics are susceptible to interception by metallo- β -lactamases, including the carbapenems, which were developed to overcome serine β -lactamase drug resistance.³ The wide variety of antibiotics that are inactivated by metallo- β -lactamases and the rising occurrence of clinical isolates of infectious bacteria containing metallo- β -lactamases have created a need for potent inhibitors of these enzymes.

Inhibitors of serine β -lactamases, such as clavulanic acid and sulbactam, are ineffective against Zn-containing β -lac-

tamases. Several classes of inhibitors of metallo- β -lactamases have been discovered, however.^{4–7} Substituted biphenyl tetrazoles competitively inhibit metallo- β -lactamase from *Bacteroides fragilis* by binding to zinc in the active site of the enzyme and disrupting a flexible β strand, or “flap”, which extends above the active site.⁴ Sulfonic acid buffers also inhibit *B. fragilis* metallo- β -lactamase, although not as strongly. The sulfonic acids interact with the active site through hydrogen bond formation and induce a conformational change in the flap.⁵ Succinic acid derivatives inhibit the IMP-1 metallo- β -lactamase enzyme by interacting with the dinuclear zinc cluster at the active site.⁸

Thiol ester derivatives and thiols also inhibit metallo- β -lactamases.^{3,6,7,9,10} Mercaptoacetic acid thiol ester derivatives

* Author to whom correspondence should be addressed. E-mail: lippard@lippard.mit.edu.

- (1) Rice, L. B.; Bonomo, R. A. *Drug Resist. Updates* **2000**, *3*, 178–189.
- (2) Cricco, J. A.; Orellano, E. G.; Rasia, R. M.; Ceccarelli, E. A.; Vila, A. J. *Coord. Chem. Rev.* **1999**, *190–192*, 519–535.
- (3) Greenlee, M. L.; Laub, J. B.; Balkovec, J. M.; Hammond, M. L.; Hammond, G. G.; Pompliano, D. L.; Epstein-Toney, J. H. *Bioorg. Med. Chem. Lett.* **1999**, *9*, 2549–2554.

- (4) Toney, J. H.; Fitzgerald, P. M. D.; Grover-Sharma, N.; Olson, S. H.; May, W. J.; Sundelof, J. G.; Vanderwall, D. E.; Cleary, K. A.; Grant, S. K.; Wu, J. K.; Kozarich, J. W.; Pompliano, D. L.; Hammond, G. G. *Chem. Biol.* **1998**, *5*, 185–196.
- (5) Fitzgerald, P. M. D.; Wu, J. K.; Toney, J. H. *Biochemistry* **1998**, *37*, 6791–6800.
- (6) Payne, D. J.; Bateson, J. H.; Gasson, B. C.; Proctor, D.; Khushi, T.; Farmer, T. H.; Tolson, D. A.; Bell, D.; Skett, P. W.; Marshall, A. C.; Reid, R.; Ghosez, L.; Combret, Y.; Marchand-Brynaert, J. *Antimicrob. Agents Chemother.* **1997**, *41*, 135–140.
- (7) Goto, M.; Takahashi, T.; Yamashita, F.; Koreeda, A.; Mori, H.; Ohta, M.; Arakawa, Y. *Biol. Pharm. Bull.* **1997**, *20*, 1136–1140.

irreversibly inhibit metallo- β -lactamase from *Bacillus cereus* II. The thiol ester derivatives are hydrolyzed by the enzyme, releasing mercaptoacetic acid. The mercaptoacetic acid may then form a disulfide bond to the cysteine residue at the active site, thereby inactivating the enzyme.^{3,6,11} Thiols such as 2-mercaptoethanol decrease the activity of metallo- β -lactamase IMP-1 from *Serratia marcescens*,^{3,7} possibly also by inactivation of the active site cysteine through disulfide bond formation. Inhibition of metallo- β -lactamase with thiomandelic acid, however, proved to be reversible, indicating that there are probably several mechanisms operating for inhibition of metallo- β -lactamases by thiol-donating compounds.⁹

The postulated role of disulfide formation in the inhibitory activity of thiols and thiol esters, and previous experience with zinc–thiolate reaction chemistry in our laboratory,^{12–15} led us to consider the possibility that metallo- β -lactamases might be inactivated by thiolate–disulfide exchange. Disruption of zinc sites in proteins by disulfides is not without precedence. A series of disulfide benzamides eject zinc from the HIV-1 nucleocapsid protein NCp7. Chelation of zinc is probably disturbed owing to the formation of a disulfide bond between an active site cysteine and half of the disulfide benzamide during a thiolate–disulfide exchange.^{16,17} Zinc is also released from the protein metallothionein upon treatment with disulfides, most likely by an analogous mechanism.^{18–22} In addition, the zinc finger of replication protein A may regulate binding to ssDNA by a similar redox mechanism.²³

Despite these results and the many examples of free thiolate–disulfide exchange reactions and metal-bound thiolate reactivity in the literature,^{13,15,24–38} conclusive evidence

Table 1. Abbreviations for Zinc Thiolate Complexes (Y = (Tp^{PhMe})Zn), Thiols (Y = H), and Disulfides (Y = SC₆H₄-X) Used in the Kinetic Studies

X\Y	(Tp ^{PhMe})Zn	H	SC ₆ H ₄ -X
4-OH	3	3a	3b
4-OCH ₃	4	4a	4b
4-CH ₃	5	5a	5b
2-CH ₃	6	6a	6b
4-H	7	7a	7b
4-Cl	8	8a	8b
4-CF ₃	9	9a	9b
4-NO ₂	10	10a	10b
4-NH ₂			11b
2-NH ₂			12b
			13b

that a zinc-bound thiolate can undergo disulfide exchange is lacking. We therefore set out to determine whether such a zinc thiolate–disulfide exchange reaction would occur. In the present study, a hindered hydrotris(pyrazolyl) borate zinc thiolate complex was prepared and its exchange with a variety of disulfides was investigated. In addition, several diaryl disulfides were allowed to react with metallo- β -lactamase CcrA from *B. fragilis* and proved to be modest to strong inactivators. The results suggest a strategy for inactivating metallo- β -lactamases.

Experimental Section

General Procedure and Methods. All reagents were obtained from commercial suppliers and used without further purification. Table 1 summarizes the numbering scheme of compounds described

- (8) Toney, J. H.; Hammond, G. G.; Fitzgerald, P. M. D.; Sharma, N.; Balkovec, J. M.; Rouen, G. P.; Olson, S. H.; Hammond, M. L.; Greenlee, M. L.; Gao, Y.-D. *J. Biol. Chem.* **2001**, *276*, 31913–31918.
- (9) Mollard, C.; Moali, C.; Papamicael, C.; Damblon, C.; Vesslier, S.; Amicosante, G.; Schofield, C. J.; Galleni, M.; Frère, J.-M.; Roberts, G. C. K. *J. Biol. Chem.* **2001**, *276*, 45015–45023.
- (10) Concha, N. O.; Janson, C. A.; Rowling, P.; Pearson, S.; Cheever, C. A.; Clarke, B. P.; Lewis, C.; Galleni, M.; Frère, J.-M.; Payne, D. J.; Bateson, J. H.; Abdel-Meguid, S. S. *Biochemistry* **2000**, *39*, 4288–4298.
- (11) Materon, I. C.; Palzkill, T. *Protein Sci.* **2001**, *10*, 2556–2565.
- (12) Wilker, J. J.; Lippard, S. J. *J. Am. Chem. Soc.* **1995**, *117*, 8682–8683.
- (13) Wilker, J. J.; Wetterhahn, K. E.; Lippard, S. J. *Inorg. Chem.* **1997**, *36*, 2079–2083.
- (14) Wilker, J. J.; Lippard, S. J. *Inorg. Chem.* **1997**, *36*, 969–978.
- (15) Wilker, J. J.; Lippard, S. J. *Inorg. Chem.* **1999**, *38*, 3569–3574.
- (16) Tummino, P. J.; Harvey, P. J.; McQuade, T.; Domagala, J.; Gogliotti, R.; Sanchez, J.; Song, Y.; Hupe, D. *Antimicrob. Agents Chemother.* **1997**, *41*, 394–400.
- (17) Topol, I. A.; McGrath, C.; Chertova, E.; Dasenbrock, E.; Lacourse, W. R.; Eissenstat, M. A.; Burt, S. K.; Henderson, L. E.; Casas-Finet, J. R. *Protein Sci.* **2001**, *10*, 1434–1445.
- (18) Maret, W. *Proc. Natl. Acad. Sci. U.S.A.* **1994**, *91*, 237–241.
- (19) Jiang, L.-J.; Maret, W.; Vallee, B. L. *Proc. Natl. Acad. Sci. U.S.A.* **1998**, *95*, 3483–3488.
- (20) Maret, W. *Neurochem. Int.* **1995**, *27*, 111–117.
- (21) Jacob, C.; Maret, W.; Vallee, B. L. *Proc. Natl. Acad. Sci. U.S.A.* **1998**, *95*, 3489–3494.
- (22) Maret, W.; Larsen, K. S.; Vallee, B. L. *Proc. Natl. Acad. Sci. U.S.A.* **1997**, *94*, 2233–2237.
- (23) Park, J.-S.; Wang, M.; Park, S.-J.; Lee, S.-M. *J. Biol. Chem.* **1999**, *274*, 29075–29080.
- (24) Kuehn, C.; Isied, S. S. *Prog. Inorg. Chem.* **1979**, *27*, 153–221.
- (25) Deutsch, E.; Root, M. J.; Nosco, D. L. *Adv. Inorg. Bioinorg. Mech.* **1982**, *269*–389.

- (26) Singh, R.; Whitesides, G. M. In *The Chemistry of Sulphur-Containing Functional Groups*; Patai, S.; Rappoport, Z., Eds.; John Wiley & Sons Ltd.: New York, 1993; pp 633–658.
- (27) Singh, R.; Whitesides, G. M. *J. Am. Chem. Soc.* **1990**, *112*, 1190–1197.
- (28) Houk, J.; Whitesides, G. M. *J. Am. Chem. Soc.* **1987**, *109*, 6825–6836.
- (29) Whitesides, G. M.; Lilburn, J. E.; Szajewski, R. P. *J. Org. Chem.* **1977**, *42*, 332–338.
- (30) Pleasants, J. C.; Guo, W.; Rabenstein, D. L. *J. Am. Chem. Soc.* **1989**, *111*, 6553–6558.
- (31) Whitesides, G. M.; Houk, J.; Patterson, M. A. K. *J. Org. Chem.* **1983**, *48*, 112–115.
- (32) Houk, J.; Singh, R.; Whitesides, G. M. *Methods Enzymol.* **1987**, *143*, 129–140.
- (33) DePamphilis, B. V.; Averill, B. A.; Herskovitz, T.; Que, L., Jr.; Holm, R. H. *J. Am. Chem. Soc.* **1974**, *96*, 4161–4162.
- (34) Treichel, P. M.; Rublein, E. K. *J. Organomet. Chem.* **1992**, *423*, 391–398.
- (35) Brand, U.; Rombach, M.; Vahrenkamp, H. *Chem. Commun.* **1998**, 2717–2718.
- (36) Nakayama, H.; Prout, K.; Hill, H. A. O.; Datta, D. *Chem. Commun.* **1999**, 695–696.
- (37) Brand, U.; Rombach, M.; Seebacher, J.; Vahrenkamp, H. *Inorg. Chem.* **2001**, *40*, 6151–6157.
- (38) DiLorenzo, M.; Ganesh, S.; Tadayon, L.; Chen, J.; Bruce, M. R. M.; Bruce, A. E. *Metal Based Drugs* **1999**, *6*, 247–253.

in the text. ^1H NMR spectra were obtained on a Varian Unity 300 MHz spectrometer at 24 °C. Deuterated benzyl mercaptan (BzSH- d_7) was prepared according to a literature procedure from d_7 -benzyl chloride (Aldrich) and thiourea in ethanol, followed by alkaline hydrolysis (43% yield).³⁹ It was stored at -20 °C under dinitrogen. Deuterated solvents were obtained from Cambridge Isotope Laboratories (CIL) and used without further purification. Disulfides where a synthesis is not explicitly described in the text were either obtained commercially from Aldrich or donated by Merck. **CAUTION: The syntheses and procedures described below involve compounds that contain the perchlorate ion, which can detonate explosively and without warning. Although we have not encountered any problems with the reported compounds, all due precautions should be taken.**

Synthesis of $[\text{Zn}(\text{Tp}^{\text{PhMe}})(\text{OH})]$ (1a**) and $[\text{Zn}(\text{Tp}^{\text{PhMe}})(\text{OCH}_3)] \cdot 2\text{CH}_3\text{OH}$ (**1b**· $2\text{CH}_3\text{OH}$).** A literature procedure for obtaining this compound was followed with modifications.⁴⁰ To a solution of $\text{K}(\text{Tp}^{\text{PhMe}})$ (1.008 g, 1.929 mmol) in methylene chloride (50 mL) was added $\text{Zn}(\text{ClO}_4)_2 \cdot 6\text{H}_2\text{O}$ (718 mg, 1.93 mmol) in methanol (10 mL). The solution immediately turned from clear and colorless to cloudy and white. The solution was stirred for 15 min, after which KOH powder (146 mg, 2.60 mmol) was added. The reaction mixture was stirred for an additional 44 h. The KClO_4 precipitate was removed by filtration, and the volume of the filtrate was reduced. The remaining white residue was washed with MeOH and dried in high vacuum to afford 286 mg (25.6% based on $\text{K}(\text{Tp}^{\text{PhMe}})$) of **1a**. X-ray quality colorless crystals of **1b**· $2\text{CH}_3\text{OH}$ were obtained as a minor byproduct by recrystallization from methanol at -30 °C. **1a**: ^1H NMR (CDCl_3): δ 2.55 (s, 9H, CH_3 pz), 6.27 (s, 3H, H pz), 7.325–7.40 (m, 9H, Ph(3,4,5) pz), 7.79 (d, 6H, Ph(2,6) pz). Anal. Calcd for **1b**: C, 64.22; H, 5.39; N, 14.49. Found: C, 63.97; H, 5.38; N, 14.37.

Synthesis of $[\text{Zn}(\text{Tp}^{\text{PhMe}})(\text{SCH}_2\text{C}_6\text{H}_5)]$ (2**) and Related Thiolate Complexes (**3–10**).** A literature procedure for obtaining **2** was followed with modifications.⁴¹ A solution of **1a** (200 mg, 0.345 mmol) in 6 mL of methylene chloride was added to a solution of benzyl mercaptan (**2a**, 42 mg, 0.34 mmol) in 12 mL of methanol. The resulting solution was stirred overnight, and the solvents were removed by slow evaporation at room temperature. The crystalline residue was carefully washed with methanol, yielding 100 mg (44% based on **1**) of $[\text{Zn}(\text{Tp}^{\text{PhMe}})(\text{SCH}_2\text{C}_6\text{H}_5)]$ (**2**). ^1H NMR ($\text{DMSO}-d_6$): δ 2.07 (s, 2H, CH_2), 2.56 (s, 9H, CH_3 pz), 6.36 (d, 2H, $\text{CH}_2\text{Ph}(2,6)$), 6.46 (s, 3H, H pz), 7.00 (m, 3H, $\text{CH}_2\text{Ph}(3,4,5)$), 7.41–7.43 (m, 9H, Ph(3,4,5) pz), 7.73–7.77 (m, 6H, Ph(2,6) pz). Anal. Calcd for **2**: C, 66.13; H, 5.25; N, 12.51. Calcd for **2**· $0.5\text{H}_2\text{O}$: C, 65.26; H, 5.33; N, 12.34. Found: C, 65.66; H, 5.35; N, 12.34. Compounds **3–10** were prepared in a similar manner and isolated after slow evaporation of the solvent at room temperature as colorless crystals except for **10**, which is yellow. Table S1 (Supporting Information) summarizes the ^1H NMR spectroscopic features of **3–10** in CDCl_3 and $\text{DMSO}-d_6$.

Synthesis of Disulfides. Bis(4-hydroxyphenyl) Disulfide (3b**), Bis(4-methoxyphenyl) Disulfide (**4b**), Bis(4-tolyl) Disulfide (**5b**), Bis(2-tolyl) Disulfide (**6b**), Bis(4-chlorophenyl) Disulfide (**8b**), Bis(4-trifluoromethylphenyl) Disulfide (**9b**), and Bis(4-nitrophenyl) Disulfide (**10b**).** Methods for preparing diaryl disulfides by oxidation of the corresponding thiol by DMSO can be found in the literature.^{42–44} 4-Nitrobenzenethiol (**10a**, 2.001 g, 0.01290 mol)

was dissolved in dimethyl sulfoxide (32 mL, 0.45 mol) to afford a red-orange solution, which was heated at 90 °C for 21 h, cooled, and poured into 500 mL of ice water. Filtration of the resulting precipitate produced a yellow powder, bis(4-nitrophenyl) disulfide (**10b**) (1.904 g, 95.7%). ^1H NMR of **10b** ($\text{DMSO}-d_6$): δ 7.80 (d, 2H, Ph(2,6)), 8.24 (d, 2H, Ph(3,5)). Anal. Calcd for $\text{C}_{12}\text{H}_8\text{N}_2\text{O}_4\text{S}_2$: C, 46.75; H, 2.62; S, 20.80. Found: C, 45.92; H, 2.26; S, 20.15. A similar procedure was followed for the syntheses of bis(4-trifluoromethylphenyl) disulfide (**9b**), bis(4-chlorophenyl) disulfide (**8b**) (1.62 g, 81.8%), bis(4-tolyl) disulfide (**5b**) (0.823 g, 83%), bis(4-methoxyphenyl) disulfide (**4b**), and bis(4-hydroxyphenyl) disulfide (**3b**). Crude bis(4-trifluoromethylphenyl) disulfide (**9b**) was recrystallized from *n*-propanol/water (0.72 g, 48%). ^1H NMR of bis(4-trifluoromethylphenyl) disulfide (**9b**) ($\text{DMSO}-d_6$): δ 7.75 (m, 8H, Ph). Anal. Calcd for $\text{C}_{14}\text{H}_8\text{F}_6\text{S}_2$: C, 47.46; H, 2.28; S, 18.10. Found: C, 47.44; H, 2.04; S, 17.69. ^1H NMR of bis(4-chlorophenyl) disulfide (**8b**) ($\text{DMSO}-d_6$): δ 7.44 (d, 4H, Ph(2,6)), 7.52 (d, 4H, Ph(3,5)). Anal. Calcd for $\text{C}_{12}\text{H}_8\text{S}_2\text{Cl}_2$: C, 50.18; H, 2.81; S, 22.32. Found: C, 50.14; H, 2.60; S, 21.89. ^1H NMR of bis(4-tolyl) disulfide (**5b**) ($\text{DMSO}-d_6$): δ = 2.28 (s, 6H, CH_3), 7.18 (d, 4H, Ph(3,5)), 7.38 (d, 4H, Ph(2,6)). Anal. Calcd for $\text{C}_{14}\text{H}_{14}\text{S}_2$: C, 68.25; H, 5.73; S, 26.02. Found: C, 68.10; H, 5.75; S, 26.03. Crude bis(4-methoxyphenyl) disulfide (**4b**) was purified by recrystallization from ethanol. ^1H NMR of bis(4-methoxyphenyl) disulfide (**4b**) (CDCl_3): δ 3.81 (s, 6H, CH_3), 6.84 (d, 4H, Ph(3,5)), 7.41 (d, 4H, Ph(2,6)). Crude bis(4-hydroxyphenyl) disulfide (**3b**) was purified by recrystallization from toluene/pentane (0.771 g, 50.1%). ^1H NMR of bis(4-hydroxyphenyl) disulfide (**3b**) ($\text{DMSO}-d_6$): δ 6.73 (d, 4H, Ph(3,5)), 7.24 (d, 4H, Ph(2,6)), 9.82 (s, 2H, OH). Anal. Calcd for $\text{C}_{12}\text{H}_{10}\text{O}_2\text{S}_2$: C, 57.58; H, 4.03; S, 25.61. Found: C, 57.53; H, 3.99; S, 25.32. 2-Methylbenzenethiol (**6a**) (0.8 g, 6.1 mmol) was dissolved in dimethyl sulfoxide (10 mL, 0.14 mol) to afford a pale yellow solution, which was stirred for 24 h at room temperature. Addition of ethanol allowed isolation of a yellow oil, which started to crystallize out at -20 °C. The colorless crystals were washed with cold ethanol and dried under high vacuum (200 mg, 26%). ^1H NMR of bis(2-tolyl) disulfide (**6b**) (CDCl_3): δ 2.44 (s, 6H, CH_3), 7.16 (m, 6H, Ph(3,4,5)), 7.55 (m, 2H, Ph(2)).

X-ray Crystallography. Data were collected on a Bruker (formerly Siemens) CCD X-ray diffractometer controlled by a Pentium-based PC running the SMART software package.⁴⁵ Single crystals were mounted on the tips of glass fibers with Paratone N (Exxon) and cooled to -80 or -85 °C. The general procedures for data collection and reduction followed those reported previously.⁴⁶ Empirical absorption corrections were calculated and applied from the SADABS program.⁴⁷ Structures were solved by the direct methods program XS, and refinements were carried out with XL, both part of the SHELXTL program package.⁴⁸ Structures were checked with the PLATON program for higher symmetry.⁴⁹ Non-hydrogen atoms were refined by a series of least-squares cycles. All hydrogen atoms except in **3**, **7**, and **9** were assigned idealized positions and given a thermal parameter 1.2 times the thermal parameter of the carbon atom to which each was attached.

(42) Wallace, T. J. *J. Am. Chem. Soc.* **1964**, *86*, 2018–2021.

(43) Wallace, T. J.; Weiss, H. A. *Chem. Ind.* **1966**, 1558–1559.

(44) Fristad, W. E.; Peterson, J. R. *Synth. Commun.* **1985**, *15*, 1–5.

(45) SMART V5.625; Bruker AXS, Inc.; Madison WI, 2000.

(46) Feig, A. L.; Bautista, M. T.; Lippard, S. J. *Inorg. Chem.* **1996**, *35*, 6892–6898.

(47) Sheldrick, G. M. *SADABS v2.03: Area-Detector Absorption Correction*; University of Göttingen: Göttingen, Germany, 1996.

(48) Sheldrick, G. M. *SHELXL97-2: Program for the Refinement of Crystal Structures*; University of Göttingen: Göttingen, Germany, 1997.

(49) Spek, A. L. *PLATON, A Multipurpose Crystallographic Tool*; Utrecht University: Utrecht, The Netherlands, 1998.

(39) Autorenkollektiv *Organikum*, 18th ed.; Deutscher Verlag der Wissenschaften: Berlin, 1990.

(40) Ruf, M.; Vahrenkamp, H. *Inorg. Chem.* **1996**, *35*, 6571–6578.

(41) Burth, R.; Vahrenkamp, H. *Z. Anorg. Allg. Chem.* **1998**, *624*, 381–385.

Table 2. Summary of X-ray Crystallographic Data

	1b ·2CH ₃ OH	2	3	7	9	10	13
formula	C ₃₃ H ₃₉ BN ₆ O ₃ Zn	C ₃₇ H ₃₅ BN ₆ SZn	C ₃₇ H ₃₇ BN ₆ O ₂ SZn	C ₃₆ H ₃₃ BN ₆ SZn	C ₃₈ H ₃₄ BCl ₂ F ₃ N ₆ SZn	C ₃₇ H ₃₄ BCl ₂ N ₇ O ₂ SZn	C ₃₅ H ₃₂ BN ₇ SZn
fw	643.88	671.95	705.97	657.92	810.85	750.81	658.92
cryst system	monoclinic	triclinic	triclinic	monoclinic	monoclinic	triclinic	monoclinic
space group	<i>P</i> 2 ₁ / <i>n</i>	<i>P</i> $\bar{1}$	<i>P</i> $\bar{1}$	<i>P</i> 2 ₁ / <i>n</i>	<i>C</i> 2/ <i>c</i>	<i>P</i> $\bar{1}$	<i>P</i> 2 ₁ / <i>c</i>
<i>a</i> , Å	10.091(5)	11.699(5)	11.966(2)	19.478(2)	30.11(2)	14.028(3)	11.1178(4)
<i>b</i> , Å	12.925(5)	12.515(5)	12.276(2)	11.1977(13)	11.604(8)	16.398(3)	12.5078(2)
<i>c</i> , Å	25.860(5)	13.388(5)	13.119(2)	30.012(4)	25.342(18)	17.664(4)	22.9924(6)
α , deg		69.084(5)	114.226(3)			87.912(4)	
β , deg	100.307(5)	71.052(5)	99.203(3)	96.416(2)	121.096(12)	70.601(4)	90.148(2)
γ , deg		72.267(5)	90.094(3)			71.961(4)	
<i>V</i> , Å ³	3318(2)	1691.9(12)	1729.9(5)	6504.9(13)	7582(9)	3634.2(12)	3197.30(15)
<i>Z</i>	4	2	2	8	8	4	4
<i>T</i> , K	188(2)	188(2)	193(2)	193(2)	193(2)	193(2)	188(2)
ρ_{calc} , g cm ⁻³	1.289	1.319	1.355	1.344	1.421	1.440	1.369
$\mu(\text{Mo K}\alpha)$, mm ⁻¹	0.782	0.823	0.813	0.855	0.895	0.925	0.871
2 θ range, deg	3–46	3–46	3–57	3–57	3–57	2–57	3–46
total no. of data	20392	10677	10777	39740	23141	33536	19683
no. of unique data	7668	7449	7518	14804	8702	16620	7437
no. of obsd data	5195	4700	5910	9937	6699	6365	5844
no. of params	404	423	576	1075	610	927	414
<i>R</i> ^{<i>a,b</i>}	0.0464	0.0447	0.0327	0.0381	0.0409	0.0848	0.0320
wR2 ^{<i>a,c</i>}	0.1289	0.1086	0.0801	0.0779	0.1027	0.1841	0.0784

^a Observation criterion: $I > 2\sigma(I)$. ^b $R = \sum ||F_o - F_c| / \sum |F_o|$. ^c wR2 = $\{\sum [w(F_o^2 - F_c^2)^2] / \sum [w(F_o^2)^2]\}^{1/2}$.

Experimental details are provided in Table 2. The phenyl group was disordered and modeled over two positions, each with 50% occupancy. In the structure of **9**, the dichloromethane solvent is located on a special position. All pertinent crystallographic information for each complex, including bond distances and angles, atomic coordinates, and equivalent isotropic displacement parameters, is provided in Tables S2–S36 in the Supporting Information.

Disulfide Exchange Reactions. Exchange reactions were examined of **2** with bis(4-hydroxyphenyl) disulfide (**3b**), bis(4-methoxyphenyl) disulfide (**4b**), bis(4-tolyl) disulfide (**5b**), bis(2-tolyl) disulfide (**6b**), diphenyl disulfide (**7b**), bis(4-chlorophenyl) disulfide (**8b**), bis(4-trifluoromethylphenyl) disulfide (**9b**), bis(4-aminophenyl) disulfide (**11b**), bis(2-aminophenyl) disulfide (**12b**), and 2,2'-dipyridyl disulfide (**13b**). Diethyl disulfide was used as an aliphatic substrate, but reacted only very slowly with **2**, no reaction occurring after several hours. Solutions of **2** and the disulfides were freshly prepared before each set of experiments and maintained at 24 °C in the dark. The reaction was initiated by addition of the disulfide solution to the solution of **2**, followed by thorough mixing. Times between the start of the reaction and data collection ranged between 2 and 4 min. In a representative NMR experiment, 0.4 mL of a 19.0 mM solution of **2** in DMSO-*d*₆ was mixed in an NMR tube with 0.4 mL of a 19.0 mM solution of the disulfide in DMSO-*d*₆. The progress of the reaction was monitored by ¹H NMR spectroscopy at 24 °C by following the increase of the intensity of the Ph–CH₂–S–S–Ar peak at ~4 ppm. Every reaction was repeated at least twice, and deviations were generally less than 10%. The program Kaleidagraph was used to determine kinetic parameters and their uncertainties. Initial rates were used to calculate rate constants for slow reactions (10–15% completion); fast reactions (> 15% completion after 15–20 min of monitoring the reaction) were analyzed by using integrated rate laws. Rate constants obtained by integration were transformed into initial rates to allow direct comparison of kinetic parameters.

Isolation of the Dipyridyl Disulfide Exchange Product, [Zn-(Tp^{PhMe})(SC₃H₄N)] (13**).** Solutions of **2** (0.048 g, 0.0714 mmol) and 2,2'-dipyridyl disulfide (**13b**) (0.016 g, 0.0726 mmol), each in 3 mL of dimethyl sulfoxide, were mixed. The resulting solution was stirred overnight and then heated at 55 °C for 8 h. The mixture

was cooled and concentrated under vacuum. The resulting solution produced X-ray quality crystals within 3 days at room temperature. ¹H NMR of **13** (DMSO-*d*₆): δ 2.56 (s, 9H, CH₃ pz), 5.96 (dd, 1H, Pyr(4)), 6.39 (s, 3H, H pz), 6.44 (d, 1H, Pyr(3)), 6.70 (d, 1H, Pyr(5)), 6.79 (dd, 1H, Pyr(6)), 7.09 (m, 9H, Ph(3,4,5) pz), 7.60 (m, 6H, Ph(2,6) pz). Anal. Calcd for **13**: C, 63.80; H, 4.89; N, 14.88. Found: C, 63.69; H, 5.04; N, 15.43.

Expression and Purification of Metallo- β -lactamase IMP-1 from *Pseudomonas aeruginosa* and CcrA from *B. fragilis*. The recombinant plasmid pET30a+ was transformed into *Escherichia coli* BL21(DE3) cells by electroporation. The IMP-1 enzyme was expressed and purified according to literature procedures.^{50,51} The CcrA enzyme was expressed and purified by Dr. Natalia Kamin-skaia in our laboratory according to a published procedure.⁵² Kinetic parameters for the hydrolysis of nitrocefin were monitored at 490 nm at 25 °C, by using a Cary 1E spectrophotometer equipped with a temperature control unit. The reactions were performed in a total volume of 1 mL in 50 mM MOPS, pH 7.0. The zinc content of the protein solution was determined to be 1.07×10^{-7} M (AAS). The assay medium of IMP-1 also contained 2 mM CHAPS.⁵⁰ Solutions of the inhibitors and nitrocefin were freshly prepared in DMSO. The steady-state kinetic parameters K_M and k_{cat} were derived from initial velocity measurements by using the computer programs Kaleidagraph and Origin. Absorbance data were converted into concentrations by using an extinction coefficient ϵ_{490} of $16\,000\text{ M}^{-1}\text{ cm}^{-1}$ for nitrocefin. The data obtained were from three independent experiments. Kinetic parameters are in good accord with previously published values.^{11,53}

Inhibition Studies of CcrA with Disulfides. The disulfides were tested for inhibition in the following manner. The protein (10^{-7} M

- (50) Hammond, G. G.; Huber, J. L.; Greenlee, M. L.; Laub, J. B.; Young, K.; Silver, L. L.; Balkovec, J. M.; Pryor, K. D.; Wu, J. K.; Leiting, B.; Pompliano, D. L.; Toney, J. H. *FEMS Microbiol. Lett.* **1999**, *459*, 289–296.
 (51) Pryor, K. D.; Leiting, B. *Protein Expression Purif.* **1997**, *10*, 309–319.
 (52) Toney, J. H.; Wu, J. K.; Overbye, K. M.; Thompson, C. M.; Pompliano, D. L. *Protein Expression Purif.* **1997**, *9*, 355–362.
 (53) Paul-Soto, R.; Hernandez-Valladares, M.; Galleni, M.; Bauer, R.; Zeppezauer, M.; Frère, J.-M.; Adolph, H.-W. *FEBS Lett.* **1998**, *438*, 137–140.

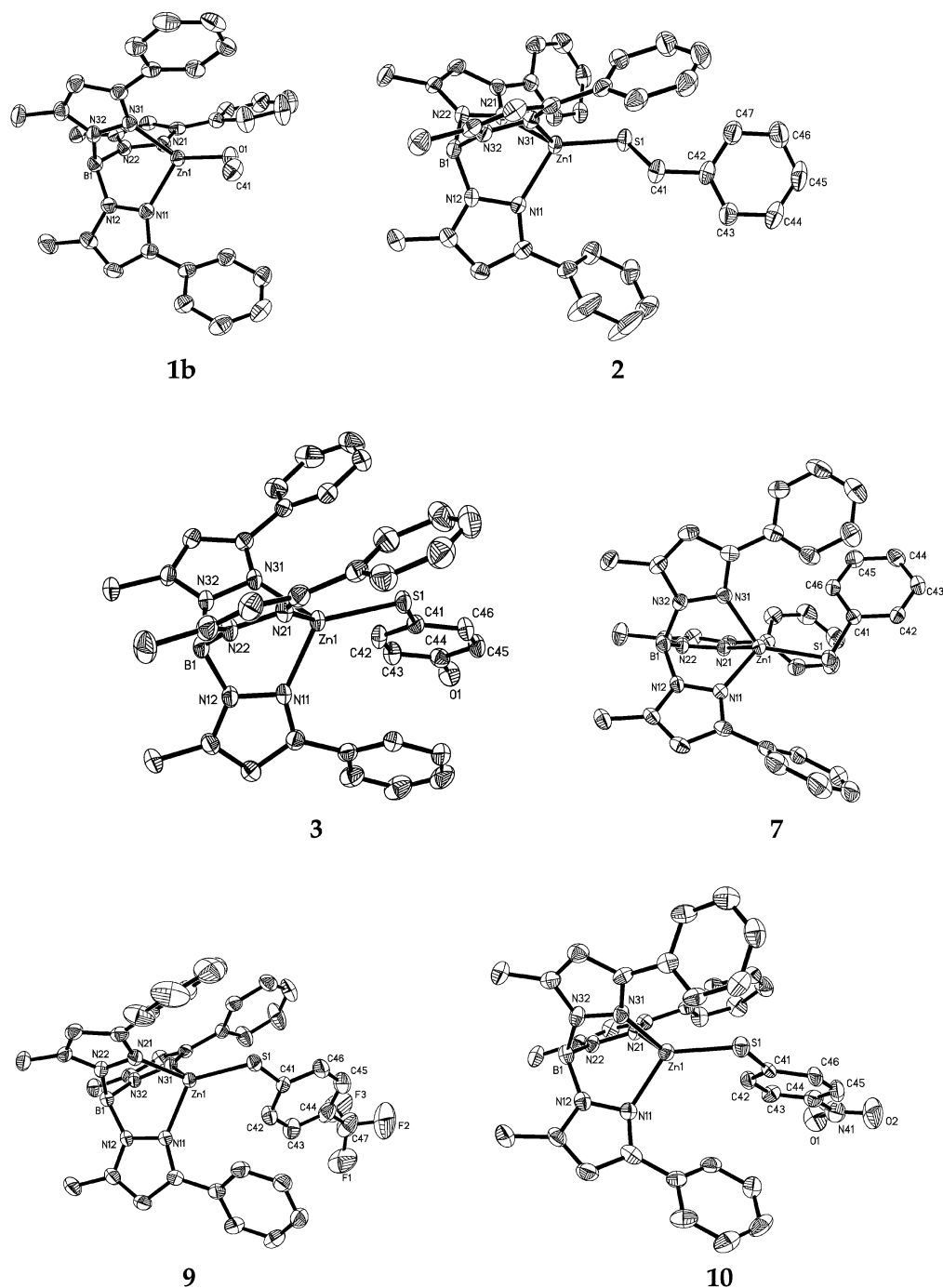


Figure 1. ORTEP diagrams of $[(\text{Tp}^{\text{PhMe}}\text{ZnOCH}_3)\cdot 2\text{CH}_3\text{OH}]$ (**1b**· $2\text{CH}_3\text{OH}$), $[(\text{Tp}^{\text{PhMe}}\text{ZnSBz})]$ (**2**), $[(\text{Tp}^{\text{PhMe}}\text{Zn}(\text{SC}_6\text{H}_4\text{OH}))]$ (**3**), $[(\text{Tp}^{\text{PhMe}}\text{Zn}(\text{SC}_6\text{H}_5))]$ (**7**), $[(\text{Tp}^{\text{PhMe}}\text{Zn}(\text{SC}_6\text{H}_4\text{CF}_3))]$ (**9**), and $[(\text{Tp}^{\text{PhMe}}\text{Zn}(\text{SC}_6\text{H}_4\text{NO}_2))]$ (**10**), showing selected atom labels and 50% probability ellipsoids for all non-hydrogen atoms and nonsolvent molecules.

in buffer) was incubated with disulfide (10^{-4} M in DMSO) at 37 °C. Just prior to the assay, the solution was diluted into disulfide-free buffer to reach a final concentration of 10^{-9} M. The assay was initiated by addition of nitrocefin to the protein solution. A blank reaction was carried out with protein that had been incubated under the same conditions (temperature, time, and DMSO concentration), except for the presence of disulfide in the medium. Disulfides leading to enzyme inhibition were scored as irreversible inhibitors, since otherwise the enzyme activity would be expected to be restored after dilution of inhibited protein into inhibitor-free medium.

Results and Discussion

Synthesis and Structural Characterization of $[\text{Zn}(\text{Tp}^{\text{PhMe}})(\text{OCH}_3)]\cdot 2\text{CH}_3\text{OH}$ (1b**· $2\text{CH}_3\text{OH}$), $[\text{Zn}(\text{Tp}^{\text{PhMe}})(\text{SCH}_2\text{C}_6\text{H}_5)]$ (**2**), and Related Thiolate Complexes $[\text{Zn}(\text{Tp}^{\text{PhMe}})(\text{SC}_6\text{H}_4\text{X})]$ (**3–10**).** The hydrotris(pyrazolyl)borate zinc complex $[\text{Zn}(\text{Tp}^{\text{PhMe}})(\text{OCH}_3)]\cdot 2\text{CH}_3\text{OH}$ (**1b**· $2\text{CH}_3\text{OH}$) was obtained as a minor byproduct in the reaction of $\text{K}(\text{Tp}^{\text{PhMe}})$ with $\text{Zn}(\text{ClO}_4)_2\cdot 6\text{H}_2\text{O}$ and KOH in a methylene chloride/methanol mixture. The sterically hindered tris-

Table 3. Selected Bond Distances (Å) and Angles (deg) for **1b**, **2**, **3**, **7**, **9**, **10**, and **13**^a

	1b	2	3	7	9	10	13
Zn–N _{av}	2.060(3)	2.072(9)	2.059(15)	2.054(2)	2.051(2)	2.058(6)	2.1110(25)
Zn–O(1)/S(1)	1.8735(19)	2.2232(11)	2.2528(6)	2.2333(8)	2.2395(15)	2.241(2)	2.3506(5)
Zn–N(40)							2.2587(15)
N(11)–Zn–N(21)	93.9(9)	90.86(10)	94.06(6)	92.12(9)	91.44(9)	93.21(23)	97.70(6)
N(21)–Zn–N(31)	92.65(9)	91.52(9)	94.61(6)	93.67(9)	91.43(8)	94.13(23)	87.07(5)
N(11)–Zn–N(31)	95.53(9)	90.39(10)	88.84(6)	90.70(8)	93.76(9)	90.62(22)	88.28(5)
N–Zn–N(av)	94.03	90.92	92.50	92.16	92.19	92.65	
N(11)–Zn–O(1)/S(1)	119.00(9)	125.41(7)	124.31(4)	128.07(6)	126.07(6)	124.36(18)	132.46(4)
N(21)–Zn–O(1)/S(1)	128.59(9)	122.54(7)	120.66(5)	114.94(6)	124.59(8)	116.51(17)	126.71(4)
N(31)–Zn–O(1)/S(1)	119.40(9)	125.85(7)	125.17(4)	127.73(6)	120.31(6)	128.53(17)	107.88(4)
N–Zn–O(av)/S(av)	123.3	124.6	123.4	123.6	123.7	123.1	
N(40)–Zn–S(1)							68.68(4)
N(11)–Zn–N(40)							99.77(5)
N(21)–Zn–N(40)							89.02(5)
N(31)–Zn–N(40)							171.46(5)

^a Numbers in parentheses are estimated standard deviations in the last significant figure. Atoms are labeled as indicated in Figures 1 and 7.

(pyrazolyl)borate ligand allows zinc to remain mononuclear and four-coordinate. The structure of the resulting complex is depicted in Figure 1. Crystallographic information is provided in Table 2, and selected bond distances and angles are reported in Table 3.

It has previously been reported that simple zinc tris(pyrazolyl)borate alkoxides are not isolable and rapidly hydrolyze to the corresponding hydroxide complex [Zn(Tp[′])(OH)].⁵⁴ Phenoxide derivatives such as [Zn(Tp^{CumMe})(OC₆H₄-*p*-NO₂)] and arylmethoxides such as [Zn(Tp^{CumMe})(OCH₂C₆F₅)] were stable and crystallizable, however. Alkoxides were more stable when electron-withdrawing groups were present, as in [Zn(Tp^{CumMe})(OCH₂CF₃)]. Recently, the structure of the ethoxide complex [Zn(Tp^{tBuMe})(OCH₂CH₃)] was described together with conditions for stabilizing the corresponding methoxide and isopropoxide compounds. The latter complexes were identified by ¹H NMR spectroscopy in the corresponding alcohol solutions, but could not be isolated therefrom. The alkoxide complexes were instead obtained from reactions of the [Zn(Tp^{tBuMe})(H)] hydride with the corresponding alcohol.⁵⁵ Despite the reported instability of **1b**·2CH₃OH, we could isolate and crystallographically analyze it as a minor byproduct in the synthesis of [(Tp^{PhMe})-ZnOH]. In the ¹H NMR spectrum obtained in DMSO-*d*₆ or CDCl₃, however, there was no evidence for bound methoxide, the CH₃O signal being unshifted compared with that of free MeOH. This result is in accord with a very small equilibrium constant and unfavorable energetics for the alcoholysis reaction of [(Tp^{PhMe})ZnOH], as determined in previous work.^{55–57}

The geometry of **1b** corresponds well with that of other zinc tris(pyrazolyl)borate alkoxides, phenoxides, arylmethoxides, and hydroxides in the literature. The Zn–O bond length

of 1.874(2) Å and the O–Zn–N angles of 119–129° in **1b** compare favorably with the Zn–O bond lengths of 1.81–1.86 Å and the O–Zn–N angles of 117–129° in the compounds [Zn(Tp^{*})(OR)] and [Zn(Tp^{*})(OH)].^{40,54,55,58}

When the zinc–hydroxide complex **1b** was treated with 1 equiv of benzyl mercaptan (**2a**) or the substituted thiophenols **3a–10a**, the corresponding tris(pyrazolyl)borate zinc thiolate complexes **2–10** were formed in moderate to very good yields. Table 2 contains crystallographic information, and selected bond distances and angles are provided in Table 3. Similar zinc thiolate complexes have been crystallographically characterized.^{41,59} The structures of the resulting complexes are shown in Figure 1. The steric hindrance of the tris(pyrazolyl)borate ligand enforces four-coordination at the zinc ion in these complexes. No polymeric species, as sometimes observed for complexes with pyrazolyl-containing ligands, could be detected. The acidity of the coordinated thiolate does not have a marked influence on the Zn–S bond lengths, which range from 2.23 to 2.25 Å, or the coordination geometry around the zinc(II) center. The average Zn–N bond length of 2.05–2.07 Å is similar to corresponding distances found in other zinc–thiolate complexes of scorpionate-type ligands.^{41,54,59–61} An average distance of 3.3–4.0 Å and a stacking angle of 2–17° between the planes of the coordinated phenylthiolate and of one of the phenyl groups of the Tp^{PhMe} ligand indicate π–π-stacking interactions.⁶² Such interactions may be important in the reactivity of **2** with disulfides, because they may assist in bringing the disulfide into a favorable position for nucleophilic attack by the zinc-coordinated thiolate. The importance of intermolecular hydrophobic interactions also emerges from the observed reactivity increase in the alkylation of zinc-bound thiolate

(54) Walz, R.; Weis, K.; Ruf, M.; Vahrenkamp, H. *Chem. Ber.* **1997**, *130*, 975–980.

(55) Bergquist, C.; Parkin, G. *Inorg. Chem.* **1999**, *38*, 422–423.

(56) Bergquist, C.; Storrie, H.; Koutcher, L.; Bridgewater, B. M.; Friesner, R. A.; Parkin, G. *J. Am. Chem. Soc.* **2000**, *122*, 12651–12658.

(57) Bräuer, M.; Anders, E.; Sinnecker, S.; Koch, W.; Rombach, M.; Brombacher, H.; Vahrenkamp, H. *Chem. Commun.* **2000**, 647–648.

(58) Alsfasser, R.; Trofimenko, S.; Looney, A.; Parkin, G.; Vahrenkamp, H. *Inorg. Chem.* **1991**, *30*, 4098–4100.

(59) Wharten, C. R.; Hammes, B. S.; Carrano, C. J.; Crans, D. C. *J. Biol. Inorg. Chem.* **2001**, 82–90.

(60) Ruf, M.; Burth, R.; Weis, K.; Vahrenkamp, H. *Chem. Ber.* **1996**, *129*, 1251–1257.

(61) Alsfasser, F.; Powell, A. K.; Trofimenko, S.; Vahrenkamp, H. *Chem. Ber.* **1993**, *126*, 685–694.

(62) Janiak, C. *J. Chem. Soc., Dalton Trans.* **2000**, 3885–3896.

in [(Tp^{PhMe})ZnSR] complexes, compared to [(Tp^{MeMe})ZnSR] complexes.³⁷ ¹H NMR spectra in CDCl₃ and DMSO-*d*₆ of compounds **2–10** indicate that the complexes retain their structures in solution, because the signals of the thiophenolate ligands are shifted to higher field compared with the corresponding resonances of the free thiol. The ¹H NMR signals of the phenyl group attached to the pyrazolyl unit reflect the electron-withdrawing properties of the substituent at the thiophenyl group. As this substituent becomes more electron-withdrawing, the signals experience a high-field shift. No signal for free thiolate or thiol is observed. Although compound [(Tp^{PhMe})ZnSC₆H₄Cl] (**8**) remains fully coordinated in CDCl₃, the complex dissociates to afford approximately 25% of its thiolate ligand in DMSO-*d*₆ (Figure S1, see Supporting Information). Given the preference of zinc(II) to form chloro complexes, and the existence of zinc chlorobenzene complexes, the phenyl moiety may interact with the zinc center via the chloride ion. Such behavior would be a first indication of the lability of the coordinated thiolate ligand, assisted by a polar solvent.

Lability of the Coordinated Thiolate. In the literature there are contradictory reports about the lability of coordinated thiolates in scorpionate complexes.^{35,59} The ¹H NMR spectra of the present thiolate complexes in CDCl₃ and DMSO-*d*₆ are sharp and well-resolved, which could indicate either inertness or very rapid exchange. The addition of up to 10 vol % D₂O did not lead to dissociation of thiol as monitored by ¹H NMR spectroscopy. At higher concentrations, the complex starts to precipitate from solution. When an equimolar amount of CF₃COOH is added to [Zn(Tp^{PhMe})-SBz] (**2**) in DMSO-*d*₆, however, thiol is quantitatively liberated. A 2.38 mM solution of [(Tp^{PhMe})ZnSBz] (**2**) was monitored for 48 h at 25 °C, during which time 10% of the benzylthiolate ligand dissociates from **2** and is oxidized to dibenzyl disulfide.

Upon addition of thiophenols ArSH to a solution of **2** in either DMSO or CDCl₃, a mixture of the corresponding [(Tp^{PhMe})ZnSAr] complexes is formed either instantaneously in DMSO or rather slowly in CDCl₃. The relative amounts of the two complexes reflect their thermodynamic stability. The exchange reaction is first order in both thiol and **2**, which indicates that both components are involved in the rate-determining step of the exchange process in CDCl₃.

The zinc complex *d*₇-[(Tp^{PhMe})ZnSBz] (**2-d**₇) containing a fully deuterated benzyl thiolate unit was synthesized and allowed to react with HSBz and NaSBz in order to monitor the ease and rate of ligand exchange, unobscured by equilibrium shifts due to the presence of different thiols of differing p*K*_a values. Peaks corresponding to coordinated thiolate, which are absent in the deuterated compound, would indicate rapid ligand exchange.

Exchange with the thiol HSBz was observed, the exchange rate being strongly dependent on the polarity of the solvent. In apolar CDCl₃, the rate depends on the concentrations of both the zinc complex and HSBz, whereas in polar DMSO exchange occurs instantly. Again, a second-order dependence can be interpreted as evidence that both the zinc thiolate complex and HSBz are involved in the rate-determining step

of the exchange reaction in CDCl₃, pointing to an S_N2-like mechanism for ligand exchange in this solvent. The possibility of prior dissociation of the thiolate from [(Tp^{PhMe})ZnSBz] appears unlikely on the basis of the reaction order and the poor coordinating ability of CDCl₃ toward {(Tp^{PhMe})Zn}⁺.

The addition of sodium thiophenolates in DMSO-*d*₆, however, did not lead to fast exchange of bound BzS⁻ with ArS⁻, Ar = 4-NO₂C₆H₄ or CH₂C₆H₅. Others carried out similar experiments with [PPN]SBz and [(Tp^{PhMe})ZnSET] in CDCl₃ and reported that it took at least several weeks to reach equilibrium.^{35,37} We allowed **2-d**₇ to react with NaSBz in DMSO-*d*₆ and found that, even though exchange occurs much more rapidly in polar solvents (equilibrium can be reached in 5–10 h), it does not occur in a time frame that would account for the observed reactivity of the zinc complex. Exchange with the most active disulfides is complete within 15–30 min.

From these findings, it can be concluded that, in order to show exchange, protonation of the thiolate must occur, either by acid or a thiol of equal or higher acidity than the conjugate acid of the coordinated thiolate. Such a conclusion implies, however, that free thiolate is not kinetically competent to be the reactive species in thiolate–disulfide exchange. Instead, zinc-coordinated thiolate is responsible for the observed reactivity.

Exchange of **2 with Disulfides.** Thiolate–disulfide exchange was studied by monitoring the reaction of **2** with several aromatic disulfides at 24 °C by ¹H NMR spectroscopy in DMSO-*d*₆. Diethyl disulfide was used as an aliphatic substrate in the reaction with **2**, but reacted only very slowly.⁶³ In the reaction of **2** with diaryl disulfides (**5b**), however, the intensity of the peak at 2.076 ppm, assigned to the Zn–S–CH₂ group, decreases shortly after mixing, while simultaneously another peak at around 4 ppm grows in (Figure 2). From a comparison with authentic samples, the latter is assigned to the methylene group of the unsymmetrical disulfide Ar–S–S–CH₂–Ph, formed by oxidation of [(Tp^{PhMe})ZnSBz] with Ar–S–S–Ar. In the aromatic region, peaks around 5.8–6.4 ppm appear simultaneously. They are assigned by comparison with authentic samples to the CH(2,3) protons of the zinc-coordinated thiolate moiety Zn–S–Ar. In addition, new peaks assigned to the phenyl groups of the tris(pyrazolyl)borate ligand start to appear at slightly upfield-shifted positions compared to the corresponding signals in the benzylthiolate complex. For example, the 7.4 ppm resonance for the Ph(3,4,5) pz protons in **2** may be compared with those at 7.13–7.2 ppm in the exchange products, and the 7.75 ppm signal for Ph(2,6) pz in **2** with the 7.5–7.63 ppm values in the exchange products. After 10 min to several hours, depending on the disulfide used and on the complex-to-disulfide ratio, another peak at 3.73 ppm appeared, the intensity of which increases over time. From a comparison with an independently synthesized sample, this signal is assigned to the methylene group of the symmetrical disulfide Bz–S–S–Bz.

(63) Koeckert, M. A. M.Sc. Thesis, Massachusetts Institute of Technology, Cambridge, MA, 2000.

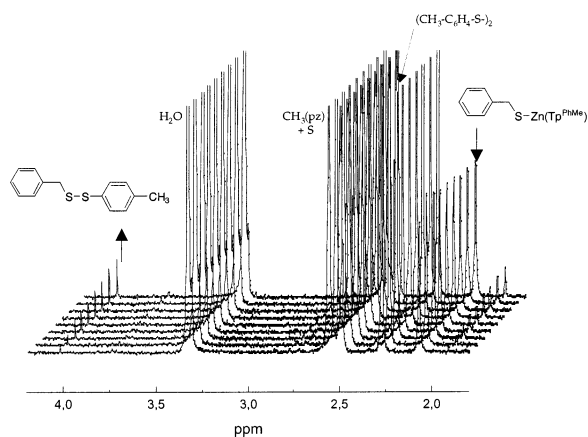
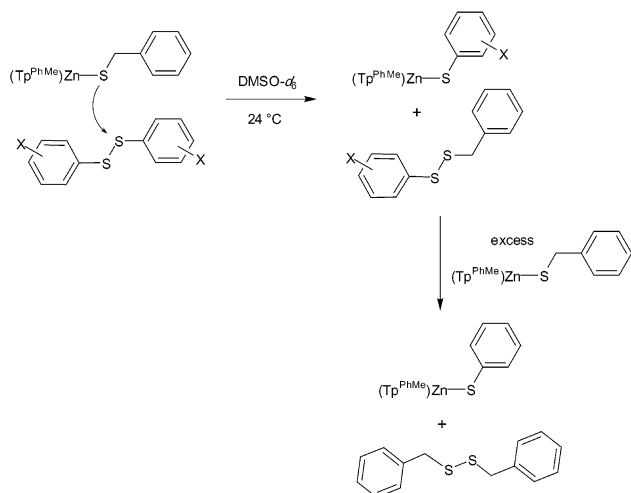


Figure 2. Monitoring the thiolate–disulfide exchange reaction by ^1H NMR spectroscopy. Focus on the gain of intensity in the 4.011 ppm signal; the corresponding decrease in the signal at 2.076 ppm is difficult to see because of its high intensity. Depicted is the reaction with bis(4-tolyl) disulfide (**5b**); the peak growing in at 1.95 ppm arises from the methyl resonance of zinc-coordinated 4-tolylthiolate. The time between the collection of each spectrum is 60 s.

Scheme 1



These NMR data reveal that a thiolate–disulfide exchange reaction between **2** and the aromatic disulfide Ar-S-S-Ar occurs (Scheme 1). The formation of the symmetric disulfide Bz-S-S-Bz indicates that the reaction proceeds further, and that the unsymmetric disulfide Ar-S-S-Bz can react with starting material $[\text{Zn}(\text{Tp}^{\text{PhMe}})\text{SBz}]$ to form Bz-S-S-Bz .

Exchange Kinetics of 2 with Disulfides. Kinetic studies of the exchange of **2** with substituted diphenyl disulfides Ar-S-S-Ar revealed the reaction to be first order in both complex and disulfide at low concentrations. Representative plots of initial rate vs concentration of $[\text{Zn}(\text{Tp}^{\text{PhMe}})\text{SBz}]$ (**2**) and [diphenyl disulfide] (**7b**) are presented in Figure 3. The observed saturation behavior at higher concentrations could arise either from the formation of an intermediate, as depicted in Scheme 2b, or dissociation of thiolate from the $[\text{Zn}(\text{Tp}^{\text{PhMe}})\text{SBz}]$ complex and subsequent reaction of free thiolate with disulfide (Scheme 2a).

If thiolate, formed by solvent-assisted cleavage (solvent = L), is assumed to be the species responsible for the observed

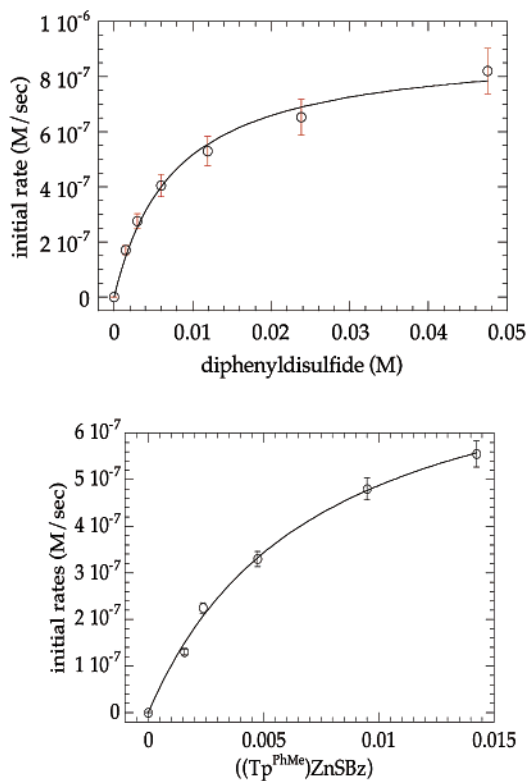


Figure 3. Plots of the initial rates of thiolate–disulfide exchange vs the concentration of diphenyl disulfide (**7b**) and **2**.

reactivity, the rate law would be described by eq 1. Saturation

$$\text{rate} = \frac{k_1[\text{ZnSR}][\text{L}]k_2[\text{S}_2]}{k_{-1}[\text{ZnL}]^+ + k_2[\text{S}_2]} \quad (1)$$

behavior with respect to zinc would occur if the first step is an equilibrium, and the rate-determining step would be nucleophilic attack of the thiolate on the disulfide, such that $k_{-1}[\text{ZnL}]^+ \gg k_2[\text{S}_2]$. Such behavior would be expected for the least reactive, that is least electrophilic, disulfides. From other studies, this result would be expected for disulfides substituted with electron-donating substituents.^{29,64–67} In the present case, however, quite the opposite behavior is observed, and such a deactivated disulfide **3a** still shows clean second-order behavior in the thiolate–disulfide exchange reaction. Saturation behavior with respect to the disulfide concentration would be expected if the first step were rate-determining. Dissociated thiolate from the zinc complex would then react very rapidly with Ar-S-S-Ar to form the mixed disulfide; that is, $k_{-1}[\text{ZnL}]^+ \ll k_2[\text{S}_2]$. We might assume such behavior to be found, if at all, for the very electrophilic disulfides; however, it is observable for the more nucleophilic **4b** with **2**. On the basis of those considerations, a mechanism involving dissociated thiolate as the reactive species does not seem likely. If we assume

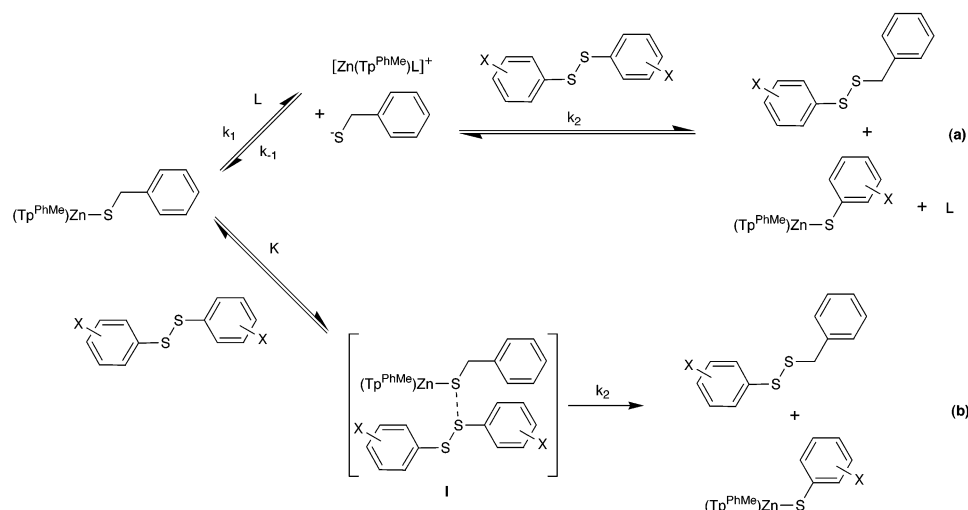
(64) Danehy, J. P.; Parameswaran, K. N. *J. Org. Chem.* **1968**, *33*, 568–572.

(65) Happer, D. A. R.; Mitchell, J. W.; Wright, G. J. *Aust. J. Chem.* **1973**, *26*, 121–134.

(66) Overman, L. E.; Matzinger, D.; O'Connor, E. M.; Overman, J. D. *J. Am. Chem. Soc.* **1974**, *96*, 6081–6089.

(67) Gilbert, H. F. *J. Am. Chem. Soc.* **1980**, *102*, 7059–7065.

Scheme 2



the reaction to proceed by intermediate I (Scheme 2b), the rate law of eq 2 would be obtained for conditions where **2** and disulfide Ar–S–S–Ar are in the same concentration range. Compound **2** and disulfide are abbreviated as A and B, respectively. Kinetic parameters obtained from fitting the

$$d[\text{Ar-S-S-Bz}]/dt = \frac{k_2 K [\text{A}][\text{B}]}{1 + K[\text{A}]} \quad (2)$$

disulfide and zinc-dependent data are in very good accord. First- and second-order rate constants, the latter being calculated for the condition that $1 \gg K[\text{A}]$, for which the rate = $k_2 K[\text{A}][\text{B}]$, are listed in Table 4a, with the association constants K . From these data it appears that disulfides bearing electron-withdrawing substituents react more rapidly than unsubstituted disulfides or disulfides having substituents with electron-donating properties. The very slow reaction of **2** with diethyl disulfide (not listed) is not surprising, for it is the most stable disulfide. Reductive cleavage of this compound would produce a thiolate more basic than benzenethiolate or the corresponding zinc complex. Such behavior would be contrary to a trend seen in the reaction of nucleophiles with disulfides, where the most acidic thiolate is the one preferentially liberated.⁶⁵

The association constant for the formation of the $[\text{Zn}(\text{Tp}^{\text{PhMe}})(\text{SBz})] \cdots [\text{Ar-S-S-Ar}]$ intermediate appears to increase with the electrophilicity of the disulfide (Table 4a). The numerical values of the association constants are small, however. *o*-Methyl substitution at the aromatic moiety has no effect on the rate of the reaction, as with results from studies on the reaction of various nucleophiles with α -substituted disulfides.^{27,66} Both of these findings disfavor the assumption of a van der Waals contact intermediate, as was postulated for the alkylation reaction of $[(\text{Tp}')\text{ZnSH}]$ and other $[(\text{Tp}')\text{ZnSR}]$ complexes with triorganophosphates.^{59,68}

Hammett plots of the first-order rate constants k against σ are depicted in Figure 4. These plots reveal that, as the substituents on the diphenyl disulfides become more electron-

withdrawing, both steps of the reaction are affected. A weakly associated $[\text{Zn}(\text{Tp}^{\text{PhMe}})(\text{SBz})] \cdots [\text{Ar-S-S-Ar}]$ complex forms in the first step, followed by breakdown to afford $[\text{Zn}(\text{Tp}^{\text{PhMe}})(\text{SAr})]$ and Bz-S-S-Ar in the second. An approximately linear Hammett correlation coefficient (slope $\rho = 1.7$) of the calculated second-order rate constants k_2 against σ (lower graph in Figure 4) indicates that the overall reaction is influenced by the electronic character of the disulfide. By analogy to the reaction of free thiols or thiolates with disulfides, attack on the S–S bond is favored when electron-withdrawing substituents activate the aromatic disulfide. The corresponding Hammett plot for the reaction of free benzyl mercaptan exhibits a slope of $\rho = 2.2$ (see below), which indicates that variation of the electronic properties of the disulfide has a similar effect on the reactivity of both **2** and **2a** with **3b–9b**. The Hammett ρ -parameter

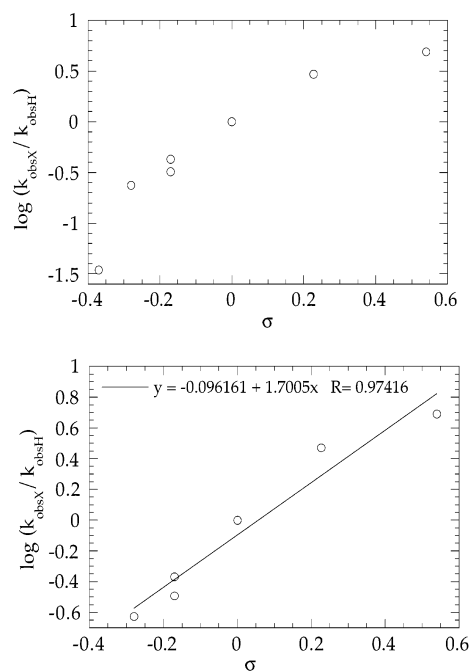
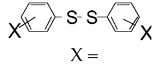
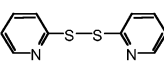


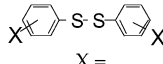
Figure 4. Hammett plot of $\log(k_{2X}/k_{2H})$ vs the Hammett constant σ . The deviant data point for bis(2-aminophenyl) disulfide is omitted in the lower plot, which allows the data to be fit to a straight line.

(68) Rombach, M.; Maurer, C.; Weis, K.; Keller, E.; Vahrenkamp, H. *Chem. Eur. J.* **1999**, *5*, 1013–1027.

Table 4. Kinetic Parameters for Exchange of **2** and **2a** with Disulfides in DMSO-*d*₆

(a) Exchange of 2 with Disulfides at 24 °C			
	Hammett constant, σ	K [M ⁻¹]	k_2 , exchange with 2 (min ⁻¹)
2-NH ₂	-0.57	96.3 ± 14.6	0.0439 ± 0.009
4-OH	-0.37	-	-
4-OCH ₃	-0.28	55.93 ± 6	0.0206 ± 0.002
4-CH ₃	-0.170	162 ± 14	0.012 ± 0.003
2-CH ₃	-0.170	158 ± 7	0.020 ± 0.002
4-H	0	133.5 ± 3.5	0.036 ± 0.001
4-Cl	0.227	306.4 ± 7.4	0.045 ± 0.001
4-CF ₃	0.54	510 ± 30	0.062 ± 0.002
	n/a	132 ± 59	0.046 ± 0.021

(b) Exchange of **2a** with Disulfides at 23 °C

	Hammett constant, σ	k [M ⁻¹ min ⁻¹]
4-NH ₂	-0.57	0.87 ± 0.03
4-OCH ₃	-0.28	0.004 ± 0.002
4-CH ₃	-0.170	0.021 ± 0.008
4-H	0	0.028 ± 0.008
4-Cl	0.227	0.107 ± 0.001
4-CF ₃	0.54	0.75 ± 0.08
4-NO ₂	0.778	1.9 ± 0.5

for the reaction of **2** and **2b** with disulfides has therefore about the same magnitude as determined for reactions of electron transfer on diaryl disulfides by aromatic radical anions ($\rho = 1.4-1.5$),⁶⁹ but is smaller than those determined for the reaction of neutral ($\rho = 2.94$)⁶⁶ and anionic nucleophiles ($\rho = 4.18$)⁶⁵ with diaryl disulfides.

The increase in k , the first-order rate constant for breakdown of the intermediate, can be explained by a weakening of the S–S-bond by electron-withdrawing substituents on the aryl ring, sensitizing the intermediate for nucleophilic attack by a zinc-coordinated thiolate. The apparent increase in K , the association constant, can be due to one or both of two effects. First, formation of a zinc-coordinated thiolate–disulfide association complex is faster when the S–S bond is weaker; second, the intermediate is stabilized with respect to dissociation to form starting material.

(69) Tagaya, H.; Aruga, T.; Ito, O.; Matsuda, M. *J. Am. Chem. Soc.* **1981**, *103*, 5484–5489.

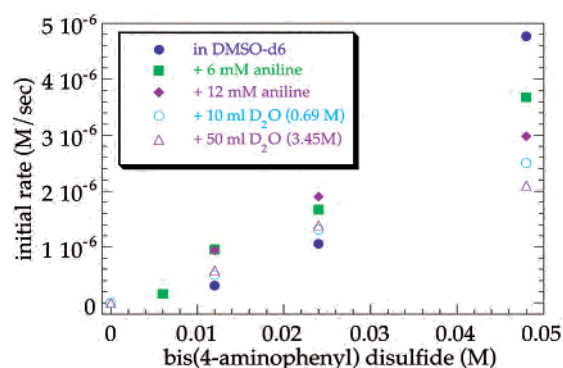


Figure 5. Plots of the initial rates of thiolate–disulfide exchange vs. the concentration of bis(4-aminophenyl) disulfide (**11b**) upon addition of aniline and D₂O, respectively.

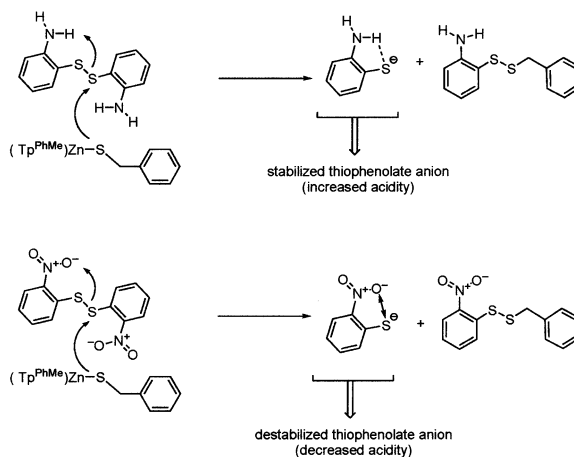


Figure 6. Proposed mechanism of the ortho activation and deactivation of diaryl disulfides.

Reaction of **2 with Bis(4-Aminophenyl) Disulfide (**11b**) and Bis(2-Aminophenyl) Disulfide (**12b**).** In the thiolate–disulfide exchange reaction of **2** and bis(4-aminophenyl) disulfide (**11b**), the results were markedly different from the ones obtained for the reaction of **2** with **3b–10b**. By analogy to the other reactions, the rate shows first-order behavior with respect to **2** at low concentrations of **2**, whereas at higher concentrations saturation behavior is observed. In contrast, the reaction exhibits second-order behavior with respect to **11b**. Upon addition of D₂O to the reaction mixture, the second-order behavior disappears and the reaction again becomes first order (Figure 5). Unlike reactions of **2** with **3b–10b**, where formation of dibenzyl disulfide is favored when an excess of **2** is present in the reaction mixture, the formation of dibenzyl disulfide is favored at high disulfide concentrations in the reaction of **2** with **11b**. The apparently different behavior is attributed to H-bonding interactions within **11b**, facilitating nucleophilic attack on **11b** by making 4-aminophenolate a better leaving group (cf. Figure 6; vide infra). Addition of D₂O leads to an increase of the rates at low disulfide concentrations, but has a negligible contribution to the reactivity at higher disulfide concentrations, or even decreases the rate under such conditions. The effect of D₂O on the rate may be due to its involvement in the H-bonding network and, therefore, in protonation of the thiolate leaving group. In order to evaluate this effect, aniline, which should mimic the ability of **11b** to participate in H-bonding, was

of both **2** and 2,2'-dipyridyl disulfide (**13b**). The data were fit to eq 2 to yield a binding constant $K = 132 \pm 59 \text{ M}^{-1}$ and an exchange rate constant $k_2 = (46 \pm 21.3) \times 10^{-3} \text{ min}^{-1}$. The second-order rate constant k_2 was calculated to be $4.78 \pm 0.12 \text{ M}^{-1} \text{ min}^{-1}$, obtained for the condition that $1 \gg K[A]$. The kinetic parameters are strikingly similar to the corresponding values observed for diphenyl disulfide **7b**, which has about the same redox potential as 2,2'-dipyridyl disulfide (**13b**).¹⁷ The observed saturation kinetics combined with the crystal structure of the exchange product⁶³ suggest that, apart from the typical hydrophobic interactions of **2** and diaryl disulfides observed in the reactions above, for 2,2'-dipyridyl disulfide the nitrogen atom of the pyridine ring may coordinate to Zn prior to exchange.

Kinetics of Exchange with Benzyl Mercaptan (2a). Kinetic studies of free thiol–disulfide exchange have been reported in the literature.^{26,27,29–32} The mechanism is believed to involve nucleophilic attack of the thiolate anion on the disulfide, with the rate of reaction depending on the concentrations of both thiol and disulfide. An addition–elimination mechanism has been proposed based on ab initio theoretical studies, however, given that the substituent on sulfur is small and allows the formation of a thiol–disulfide intermediate.⁷⁸ The rates of exchange of benzyl mercaptan with diphenyl disulfide (**7b**), bis(4-nitrophenyl) disulfide (**10b**), bis(4-aminophenyl) disulfide (**11b**), bis(4-tolyl) disulfide (**5b**), bis(4-hydroxyphenyl) disulfide (**3b**), bis(4-chlorophenyl) disulfide (**8b**), bis(4-trifluoromethylphenyl) disulfide (**9b**), and 2,2'-dipyridyl disulfide (**13b**) were determined for comparison with the exchange rates of the disulfides with **2**. Table 4b presents the observed second-order rate constants for exchange with benzyl mercaptan (**2a**) together with those for exchange with **2**. The k_2 values for the latter are in general 20–200 times greater than the values for exchange with benzyl mercaptan (**2a**), with the exception of 2,2'-dipyridyl disulfide (**13b**). A Hammett plot constructed for exchange with benzyl mercaptan reveals linear behavior with a positive slope of 2.2, as expected owing to the electron-donor or -acceptor nature of the disulfide aryl ring substituents. As these substituents become more electron-releasing, the disulfide bond becomes less activated for attack by the nucleophilic thiolate of benzyl mercaptan, causing the rate of exchange to decrease. Electron-withdrawing substituents enhance the rate of exchange by removing electron density from the disulfide bond, thus increasing its electrophilicity.

Enzyme Inactivation Studies. Among the compounds tested as potential enzyme inhibitors were several aliphatic, aromatic, and heteroaromatic disulfides (Figure 8). Only aromatic or heteroaromatic disulfides with a potential metal-binding group ortho to the disulfide moiety, or heteroaromatic systems with a para-substituted α – α' -bis-pyridine unit, were effective inhibitors, leading to irreversible inhibition of the enzyme. The parent compound 2,2'-dipyridyl disulfide, however, exhibited no activity at all. It is interesting to note

that the same reactivity pattern occurs for the inactivation of NCp7 with disulfides, although 2,2'-dipyridyl disulfide is an inhibitor in this case. Ortho activation occurs for the reasons described above, namely, intramolecular H-bonding interaction between the ortho-substituent and the thiophenolate leaving group of the disulfide, which makes it more acidic and a much better leaving group.^{17,70} Para-substitution of the diaryl disulfide may be important for steric or electronic reasons, for all the active disulfides are substituted with electron-withdrawing groups in the para position of the disulfide moiety.

Summary

A new approach is presented for inhibition of metallo- β -lactamases based on the selective oxidation of the Zn(II)-coordinated cysteine function in the active site. Zinc(II) coordination of a thiol functionality activates the thiol toward reaction with electrophiles, compared to the reactivity of the free thiol with the same reagents. The reason for such increased reactivity appears to be a consequence of the higher nucleophilicity of the zinc-coordinated thiolate compared to the thiol.

To test whether zinc coordination of cysteine 168 sufficiently activates the thiol function for selective oxidation by disulfides, disulfides were allowed to react with β -lactamase CcrA from *B. fragilis*. Aromatic disulfides with potential donor groups in close proximity to the disulfide moiety proved to be effective in inhibiting the enzyme. From mass spectrometric data it emerges that, after inhibition, the protein has undergone a mass increase corresponding to addition of at least one-half of a disulfide unit (data not shown). Such a mass increase is compatible with irreversible modification of the protein due to oxidative addition of the disulfide moiety.

These results point to a new strategy for the irreversible inhibition of β -lactamases by using sufficiently activated disulfides as selective oxidants for the metal-coordinated cysteine function.

Acknowledgment. This work was supported under the Merck/MIT Collaboration Program. B.S. thanks the Swiss National Science Foundation and the Novartis Foundation for postdoctoral support. H.B. thanks the Alexander-von-Humboldt foundation for a postdoctoral fellowship. We would like to thank Dr. Natalia Kaminskaia for helpful discussions.

Supporting Information Available: ¹H NMR spectroscopic features of **3–10** in CDCl₃ and DMSO-*d*₆, figures of ¹H NMR spectra of [(Tp^{PhMe})ZnSC₆H₄Cl] in CDCl₃ and DMSO-*d*₆ (300 MHz), X-ray crystallographic tables of complexes **1–3**, **7**, **9**, **10**, and **13**, and kinetic data for the exchange reaction of **2** with bis(4-hydroxyphenyl) disulfide (**3b**), bis(4-methoxyphenyl) disulfide (**4b**), bis(4-tolyl) disulfide (**5b**), bis(2-tolyl) disulfide (**6b**), bis(4-chlorophenyl) disulfide (**8b**), bis(4-trifluoromethylphenyl) disulfide (**9b**), bis(2-pyridyl) disulfide (**13b**), and bis(2-aminophenyl) disulfide (**12b**). Crystallographic data in CIF format. This material is available free of charge via the Internet at <http://pubs.acs.org>.

IC025624F

(78) Bachrach, S. M.; Mulhearn, D. C. *J. Phys. Chem.* **1996**, *100*, 3535–3540.